

On the transient and steady state of mass-conserved reaction diffusion systems

Shuji Ishihara¹, Mikiya Otsuji² and Atsushi Mochizuki¹

¹ Division of Theoretical Biology, National Institute for Basic Biology, 38 Nishigonaka, Myodaiji, Okazaki, Aichi, 444-8585, Japan

² Department of Anesthesiology, Faculty of Medicine, University of Tokyo, 7-3-1 Hongo, Bunkyo-ku, Tokyo 113-8655, Japan

E-mail: ishihara@nibb.ac.jp

Abstract: Reaction diffusion systems with Turing instability and mass conservation are studied. In such systems, abrupt decays of stripes follow quasi-stationary states in sequence. At steady state, the distance between stripes is much longer than that estimated by linear stability analysis at a homogeneous state given by alternative stability conditions. We show that there exist systems in which a one-stripe pattern is solely steady state for an arbitrary size of the systems. The applicability to cell biology is discussed.

Pattern formation, the emergence of a spatial structure from an initially uniform state, has been often studied on the framework of reaction diffusion systems (RDS). It is extensively applied to physical, chemical, and biological systems to explain their specific spatial structures [1, 2, 3]. Turing instability is the most prominent mechanism, forming spatially periodic stripes [4]. The intrinsic distance between stripes is, in principle, estimated by the linear stability analysis at a homogeneous state [1, 2, 3, 4]. However, this estimation could be invalid when applied far from a uniform state. For example, a second bifurcation can arise which would indicate the collapse of a simple periodic structure [5]. In such situations, the transient dynamics of pattern formation would be difficult to predict. In general, RDS shows various dynamics even when steady states are reached [6]. So far, few studies have discussed transient dynamics using the computational analysis of the famous Gray-Scott model [6, 7] and by reduced dynamics on the slow manifold [8, 9, 10].

In this Letter, we study a class of RDS in the context of the above aspects. We consider RDS showing Turing instability, in which no production and no degradation of substances occur [11]. As we will see, the following properties are observed in common; (i) The transient dynamics is a sequential transition among quasi-steady states, with a decrease in the number of stripes. (ii) The distance between resultant stripes cannot be estimated from the linear analysis at uniform state. In particular, there are systems in which a one-stripe pattern is solely stable state regardless of the system size.

Consider a diffusible chemical component with two internal states, U and V. Diffusion coefficients are D_u and D_v , respectively, for which we can set $D_u < D_v$ without loss of generality. The transition rates between U and V are regulated by each other. We studied a 1-dimensional system with size $L(0 \leq x \leq L)$ under periodic boundary conditions unless otherwise stated. Concentrations in U and V at position x and at time t are represented by $u(x, t)$ and $v(x, t)$ respectively, and obey the following equations.

$$\partial_t u = D_u \partial_x^2 u - f(u, v) \tag{1}$$

$$\partial_t v = D_v \partial_x^2 v + f(u, v) \tag{2}$$

Obviously, the total quantity of the substances (total mass) is conserved.

$$s = \frac{1}{L} \int_0^L (u + v) dx. \quad (3)$$

s is the average concentration of the substance, which is determined by the initial condition $u(x, 0)$ and $v(x, 0)$.

Below, all numerical simulations were performed with $f(u, v) = au/(b + u^2) - v$ where $s = 2.0$, $a = 1.0$, $b = 0.1$, $D_u = 0.02$, and $D_v = 1.0$. We observed qualitatively the same phenomena in several mass-conserved models [12].

Uniform state $\vec{w}^* = (u^*, v^*)$ is derived from following the conditions; $u^* + v^* = s$ and $f(u^*, v^*) = 0$ (stable fixed point in kinetic equation). Let f_u^* (f_v^*) be partial derivatives of f with regard to u (v) at \vec{w}^* . If the following relations are satisfied, uniform state \vec{w}^* loses its stability and the pattern starts to rise.

$$f_v^* < f_u^* < 0, \quad (4)$$

$$D_u f_v^* - D_v f_u^* > 0. \quad (5)$$

All the waves (e^{ikx}) with wave number k between $0 < k^2 < (D_u f_v^* - D_v f_u^*)/D_u D_v$ are unstable. At the beginning of the dynamics, the wave with the largest instability grows as in usual Turing systems (see A in Fig. 1, and the line segment representing the most unstable wavelength ℓ_m).

In a mass-conserved system, characteristic transient processes are observed. After the growth of a number of stripes (A in Fig. 1), some stripes stop growing and begin to decay (B). With the decay of a stripe, neighboring stripes grow due to mass conservation. The distance between neighboring stripes becomes larger (B-C). If the distance is large enough the state appears to reach a steady state (C, quasi-steady state). However, one (or more) stripe(s) collapses abruptly with the concomitant growth of adjacent stripes (D). As the process continues, the number of stripes decreases and the intervals between the abrupt transitions gets longer (notice the log-scale representation in Fig. 1). In Fig. 1, the system finally reaches a one-peak state. The wavelength is much larger than ℓ_m . Similar processes were observed in many mass-conserved systems.

To understand the observed transient processes, consider the stationary patterns of the system with size L . A stationary pattern $\vec{w}_0(x) = (u_0(x), v_0(x))$ is given by the solution of Eq. (1,2) with left hand sides replaced by 0. In a mass-conserved system, there is a family of stationary solutions parameterized by s , represented by $\vec{w}_0(x; s)$ explicitly. A function $h(x)$ and a value P exist, such that $u_0 = h(x)/D_u$ and $v_0(x) = (-h(x) + P)/D_v$, and satisfy the following equations.

$$P = D_u u_0(x) + D_v v_0(x) \quad (6)$$

$$\frac{d^2 h(x)}{dx^2} = f\left(\frac{h}{D_u}, \frac{-h+P}{D_v}\right) \quad (7)$$

Notice $D_u u_0(x) + D_v v_0(x)$ is independent of x . P is related to s by $P = D_v s - (D_v - D_u)\bar{h}/D_u$, in which $\bar{h} = \frac{1}{L} \int_0^L h(x) dx$ is the average of $h(x)$.

Let us represent the linear operator at a stationary state \vec{w}_0 by \mathcal{L} . There are two eigen functions belonging to the zero eigen value (0-eigen functions); $\partial_x \vec{w}_0 = (\partial_x u_0, \partial_x v_0)$ and $\partial_s \vec{w}_0 = (\partial_s u_0, \partial_s v_0)$. The former function is derived from the fact that the arbitrary translation of stationary state, $\vec{w}_0(x + \Lambda)$ is also stationary, while the latter is from the conservation property of the mass. Conjugate operator \mathcal{L}^* is defined as the transposed matrix of \mathcal{L} . One of the 0-eigen functions of this operator is $\vec{\phi}(x) = (1, 1)$. The inner product between $\vec{f} = (f^u, f^v)$ and $\vec{g} = (g^u, g^v)$ (each defined on $0 \leq x \leq L$) is to be $\langle \vec{f}, \vec{g} \rangle_L \equiv \frac{1}{L} \int_0^L (f^u g^u + f^v g^v) dx$. Then, $\vec{\phi}$ is thought to be the conjugate vector of $\partial_s \vec{w}_0$ because $\langle \vec{\phi}, \partial_s \vec{w}_0 \rangle_L = 1$ and $\langle \vec{\phi}, \partial_x \vec{w}_0 \rangle_L = 0$.

Now, to evaluate the stability of a stationary pattern, consider the following situation. Take the one-stripe stationary state \vec{w}_0 in the system with $\frac{L}{2}$ length, which takes the minimum u_0 at $x = 0 (= \frac{L}{2})$ and the maximum at $x = \frac{L}{4}$. Then copy the exact same state on $\frac{L}{2} < x < L$, and name the system on $0 \leq x \leq L$ as the non-perturbed system (NPS). Left and right halves are independent of each other. Next, the boundary condition in NPS is changed at $x = 0 (= \frac{L}{2})$ and $\frac{L}{2} (= L)$ into the usual periodic boundary condition of the system on $0 \leq x \leq L$. We refer to this modified system, which is the one we are interested in, as the perturbed system (PS). We represent the state constructed as above by $\vec{w}_0 \oplus \vec{w}_0$,

where the left (right) hand side of \oplus represents the function on $0 < x < \frac{L}{2}$ ($\frac{L}{2} < x < L$). This state is obviously a stationary solution in both NPS and PS.

Linear operators at the state are given by \mathcal{L}_0 for NPS and \mathcal{L} for PS. Because NPS is simply the juxtaposition of identical systems, $\vec{\psi}_1^0 = \partial_x \vec{w}_0 \oplus \partial_x \vec{w}_0$ and $\vec{\psi}_2^0 = \partial_s \vec{w}_0 \oplus \partial_s \vec{w}_0$ are 0-eigen functions for \mathcal{L}_0 . They are also 0-eigen functions in PS; $\mathcal{L}_0 \vec{\psi}_i^0 = \mathcal{L} \vec{\psi}_i^0 = 0$ ($i = 1, 2$). Another 0-eigen functions of \mathcal{L}_0 is $\vec{\psi}_3^0 = \partial_s \vec{w}_0 \oplus (-\partial_s \vec{w}_0)$ but this is not 0-eigen functions of \mathcal{L} anymore [18]. However, when the amplitudes of $|\partial_s u_0|$ and $|\partial_s v_0|$ are small at $x = 0$ and $\frac{L}{2}$, the discrepancy between NPS and PS is small and we can expect a function $\vec{\psi}$ and a value λ which are close to $\vec{\psi}_3^0$ and 0, respectively, and that they satisfy following relation.

$$\mathcal{L} \vec{\psi} = \lambda \vec{\psi} \quad (8)$$

If λ is positive, then the stationary state $\vec{w}_0 \oplus \vec{w}_0$ is unstable and small fluctuations grow as $\sim e^{\lambda t} \vec{\psi}$. Because $\vec{\psi}$ is similar to $\vec{\psi}_3^0 = \partial_s \vec{w}_0 \oplus (-\partial_s \vec{w}_0)$, the corresponding dynamics appears as the decay of a stripe and the growth of the other, as is observed in the numerical simulations. Note the conjugate function of $\vec{\psi}_3^0$ is $\vec{\phi}_L = \vec{\phi} \oplus (-\vec{\phi})$.

To check the validity of the above considerations, we numerically measured some related quantities. At first, we simulated the equations in the $\frac{L}{2}$ -length system and obtained a steady one-stripe state. Then, we extended the system size twice and copied the steady state to the region $\frac{L}{2} \leq x \leq L$. Next, perturbations were added keeping the total mass conserved and observed the resulting dynamics. $|\Delta s(t)| \equiv |\langle \vec{\phi}_L, \vec{w} \rangle_L| = \frac{1}{L} \left| \int_0^{\frac{L}{2}} (u+v) dx - \int_{\frac{L}{2}}^L (u+v) dx \right|$ is plotted in Fig. 2(a) which shows the exponential growth of the perturbation. Then, we compared $\vec{\psi}_3^0$ with the growing part of (u, v) . In Fig. 2(b), $\Delta \vec{w}(x) = (\Delta u(x), \Delta v(x))$ is shown, where $\Delta \vec{w}(x) = \vec{w}(x, t_2) - \vec{w}(x, t_1)$ is the difference of \vec{w} between two growing time points t_1 and t_2 . $\Delta \vec{w}(x)$ is similar to $\vec{\psi}_3^0$ which validates the above considerations.

The expected $\vec{\psi}$ is a continuous and smooth function on $0 \leq x \leq L$ and odd around $x = \frac{L}{2}$. Thus, it is enough to consider a nontrivial solution of Eq. (8) on $0 \leq x \leq \frac{L}{2}$ with boundary condition $\vec{\psi}(0) = \vec{\psi}(\frac{L}{2}) = 0$. We can limit our arguments on $0 \leq x \leq \frac{L}{2}$ in the following discussion. We properly redefine \mathcal{L} under this limitation.

To obtain $\vec{\psi}$ and λ in Eq. (8), $\vec{\psi} = \partial_s \vec{w}_0 + \vec{\eta}$ is defined. Here, $\vec{\eta} = (\eta^u, \eta^v)$ is orthogonal to $\partial_s \vec{w}_0$, i.e. $\langle \vec{\phi}, \vec{\eta} \rangle_{L/2} = 0$. In the first order of approximation, $\vec{\eta}$ satisfies the relation $\mathcal{L}\vec{\eta} = \lambda \partial_s \vec{w}_0$. The terms $m(x)$ and $Q^1(x)$ are introduced in $\eta^u(x) = m(x)/D_u$ and $\eta^v = (-m(x) + Q^1(x))/D_v$. The following equations are then obeyed.

$$\frac{d^2 Q^1}{dx^2} = \lambda (\partial_s u_0 + \partial_s v_0) \quad (9)$$

$$\frac{d^2 m}{dx^2} - \left(\frac{f_u}{D_u} - \frac{f_v}{D_v} \right) m = \frac{f_v}{D_v} Q^1(x) + \lambda \partial_s u_0 \quad (10)$$

From Eq. (9) and the boundary conditions, $Q(x) \equiv D_u \partial_s u_0 + D_v \partial_s v_0 + Q^1(x)$ is given by $Q(x) = \lambda \hat{Q}(x)$ where

$$\hat{Q}(x) = \int_0^x dx' \int_0^{x'} dx'' (\partial_s u_0(x'') + \partial_s v_0(x'')) - \frac{L}{4} x \quad (11)$$

By substituting $Q^1(x)$ into Eq. (10), $m(x) = \lambda A(x) - \partial_s P$ is obtained, where $A(x)$ is the solution of the following equation with the boundary condition $A(0) = A(\frac{L}{2}) = 0$.

$$\frac{d^2 A}{dx^2} - \left(\frac{f_u}{D_u} - \frac{f_v}{D_v} \right) A = \frac{f_v}{D_v} \hat{Q}(x) + \partial_s u_0 \quad (12)$$

Due to the orthogonality $\langle \vec{\phi}, \vec{\eta} \rangle_{L/2} = 0$, λ is given by

$$\lambda = \left(\frac{D_v - D_u}{D_u D_v} \bar{A} + \frac{1}{D_v} \bar{\hat{Q}} \right)^{-1}, \quad (13)$$

where $\bar{A} = \frac{1}{L/2} \int_0^{L/2} A(x) dx$ and $\bar{\hat{Q}} = \frac{1}{L/2} \int_0^{L/2} \hat{Q}(x) dx$.

We calculated Eq. (13) numerically. Observed growth rates and estimated values from Eq. (13) are plotted in Fig. 3 (a) against half of the system size $\frac{L}{2}$, which is the distance between two stripes. The two plots are in good agreement with each other and support the validity of the arguments presented.

From $Q(x) = \lambda \hat{Q}(x)$, we can obtain $\lambda = -\frac{4}{L} \frac{dQ(0)}{dx}$. In NPS, $Q(x)$ is given by $\partial_s P \oplus (-\partial_s P)$ and independent of x , while in PS $Q(x)$ is connected with 0 at $x = 0$ and $= \frac{L}{2}$ by the modification of boundary conditions. Thus, the sign of $\frac{dQ(0)}{dx}$ is the same as $\partial_s P$ and the sign of λ is the opposite of $\partial_s P$. This leads to the condition of two stripe instability in L -length system as

$$\partial_s P < 0. \quad (14)$$

The above arguments with the two stripes situation are extensible to an identical N -stripe pattern, where each stripe has $\frac{L}{N}$ width. Consider a set of independent functions $\vec{\Psi}_0^k = \bigoplus_{j=1}^N e^{i\frac{2\pi}{N}\kappa j} \partial_s \vec{w}_0$ ($\kappa = 1, 2, \dots, N$), where $\bigoplus_{j=1}^N$ is defined similarly to \oplus and \vec{w}_0 is redefined by the one-stripe solution of $\frac{L}{N}$ width. Then eigen functions of \mathcal{L} (redefined for the N -stripe solution), $\vec{\Psi}^\kappa$, are close to $\vec{\Psi}_0^k$. Smooth connection of $\vec{\Psi}^\kappa$ at each boundary $x = \frac{L}{N}j$ is conditioned. Consideration of $Q(x) = D_u \Psi_u^\kappa + D_v \Psi_v^\kappa$, which is close to $\bigoplus_{j=1}^N e^{i\frac{2\pi}{N}\kappa j} \partial_s P$, gives a rough estimation of the eigen values as $\lambda^\kappa \sim -4 \left(\frac{N}{L}\right)^2 \partial_s P \sin^2\left(\frac{\pi\kappa}{N}\right)$. This indicates that a shorter wave (i.e. closer κ to $\frac{N}{2}$) has larger instability if $\partial_s P < 0$. $\lambda^{\frac{N}{2}}$ for even N is identical to that estimated from two stripes. Approximated values are shown in Fig. 3. The approximated λ^1 for $N = 2$ is plotted in (a). Eigen values and corresponding eigen functions for $N = 8, L = 80.0$ are shown in (b, c).

To consider transient processes, an illustrative example can be seen from the stationary state of $2N$ -stripes with a small perturbation. If Eq. (14) is satisfied for \vec{w}_0 , the most unstable function is Ψ^N . By the growth of the perturbation along this function, the system reaches N -stripe pattern at last. If this new state becomes unstable, a similar process follows until the system reaches a steady state. In the (unstable) stationary state where the dynamics become close in their transient, λ is small if the distance between adjacent stripes is large. The corresponding state lasts for the duration of approximately λ^{-1} and therefore each state appears quasi-stationary. Because the distance becomes twice as large after each transient, the staying time in the quasi-stationary state also gets longer. We could numerically observe these processes from the 8-stripe initial condition. This demonstrates the underlying processes of the characteristic transients inherent to mass-conserved systems.

After the long transient, the system reaches the steady state at which the condition Eq. (14) is violated. Thus, the characteristic wavelength of the steady state is much longer than expected by linear stability analysis at a uniform state in a mass-conserved system. Our numerical model showed a one-stripe solution eventually between $2.0 \leq L \leq 100.0$, while $\ell_m = 3.2$ (data not shown).

Notice that Eq. (5), the condition for Turing instability, implies $\partial_s P < 0$ at the uniform

state. Therefore Eq. (14) is always satisfied in the early stages of transient, where $\vec{w}(x)$ ranges in the neighborhood of \vec{w}^* .

One interesting question that arises is the possibility of the system in which the condition in Eq. (14) is always valid in the transient quasi-steady states except in sole stripe solutions. Such systems fall into a one-stripe solution after a long transient regardless of system size. An example of such system was supplied by our group in [12], defined by $f(u, v) = -\alpha(u + v)((\delta u + v)(u + v) - \beta)$ where $\delta = D_u/D_v$. In this specific model, if L is large enough, P is well approximated by $P = \frac{3D_v\beta}{L\gamma} \frac{1}{s}$ with $\gamma \equiv \frac{1}{2} \sqrt{\frac{D_v - D_u}{D_v D_u} \alpha \beta}$. Thus a one-stripe pattern is the only stable state in the system. Though rigorous conditions are not described here, many mass-conserved systems have such properties.

In this Letter, we study RDS in which the uniform state is destabilized via a Turing mechanism and mass ($u + v$) is conserved. The analysis presented is useful for stationary patterns in any RDS and the conserved quantity does not have to be strictly defined by mass. Because the existence of any conserved quantity brings the corresponding 0-eigenfunction, our arguments are applicable. Thus, the dynamics studied here may be observed in a wider class of RDS with conserved quantities [13, 14].

We did not mention the hierarchical structure of quasi-stationary states in the phase-space, which is a necessary condition for the sequential transient as discussed in [6]. It is a global property of the phase space of the systems and difficult to study. Numerical simulations suggest it is satisfied in mass-conserved systems.

Applications of this work are possible to many phenomena, particularly to biological systems. Proposed biological models often contain conserved quantities [14, 15, 16]. At the cellular level ($\sim 10\mu m$), cytosolic proteins diffuse at $\sim 10\mu m^2/sec$ [17] leading to the rough estimation of the time scale of dynamics as $\lambda^{-1} \sim (\Delta P/L^2 \Delta s)^{-1} \sim L^2/D_v \sim 10sec$. Typically, it is faster than the synthesis or degradation of molecules and the dynamics is expected to occur within the time scale in which mass-conserved modeling is valid. The formation of cell polarity based on the above discussions is a potential application [12, 14].

S.I. is supported by Molecular-based New Computational Science Program.

- [1] G. Nicolis and I. Prigogine, *Self Organization in Non-Equilibrium Systems* (J. Wiley and Sons, New York 1977).
- [2] H. Meinhardt, *Models of Biological Pattern Formation* (Academic, New York, 1982).
- [3] J. D. Murray, *Mathematical Biology* (Springer-Verlag, Berlin, 2002), 3rd ed.
- [4] A. M. Turing, Philos. Trans. Roy. Soc. Lond. B. **237**, 37 (1952).
- [5] P. Coulet and G. Iooss, Phys. Rev. Lett. **64**, 866 (1990).
- [6] Y. Nishiura and D. Ueyama, Physica D **130**, 73 (1999); **150**, 137 (2001).
- [7] J. E. Person, Science **216**, 189 (1993).
- [8] K. Kawasaki and T. Ohta, Physica A **116**, 573 (1982).
- [9] S. Ei, Y. Nishiura, and K. Ueda, J. Dynam. Diff. Eq. **14**, 85 (2002).
- [10] T. Kolokolnikov, M. J. Ward, and J. Wei, Physica D **202**, 258 (2005).
- [11] S. Ishihara and K. Kaneko, Jour. Theor. Biol. **238**, 683 (2006).
- [12] M. Otsuji *et al.* q-bio.CB/0608025.
- [13] A. Awazu and K. Kaneko, Phy. Rev. Lett. **92**, 258302 (2004).
- [14] K. K. Subramanian and A. Narang, J. Theor. Biol. **231**, 49 (2004).
- [15] J. Keener and J. Sneyd, *Mathematical Physiology* (Springer-Verlag, New York ,1998)
- [16] K. C. Huang, Y. Meir and N. S. Wingreen, Proc. Nat. Acad. Sci. USA **100**, 12724 (2003).
- [17] M. B. Elowitz *et al.*, J. Bacteriol. **181**, 197 (1999).
- [18] $\vec{\phi}_4 = \partial_x \vec{w}_0 \oplus (-\partial_x \vec{w}_0)$ is the other independent 0-eigen function. We do not mention it for the clarity of discussion, though one can easily discuss the stability along $\vec{\phi}_4$.

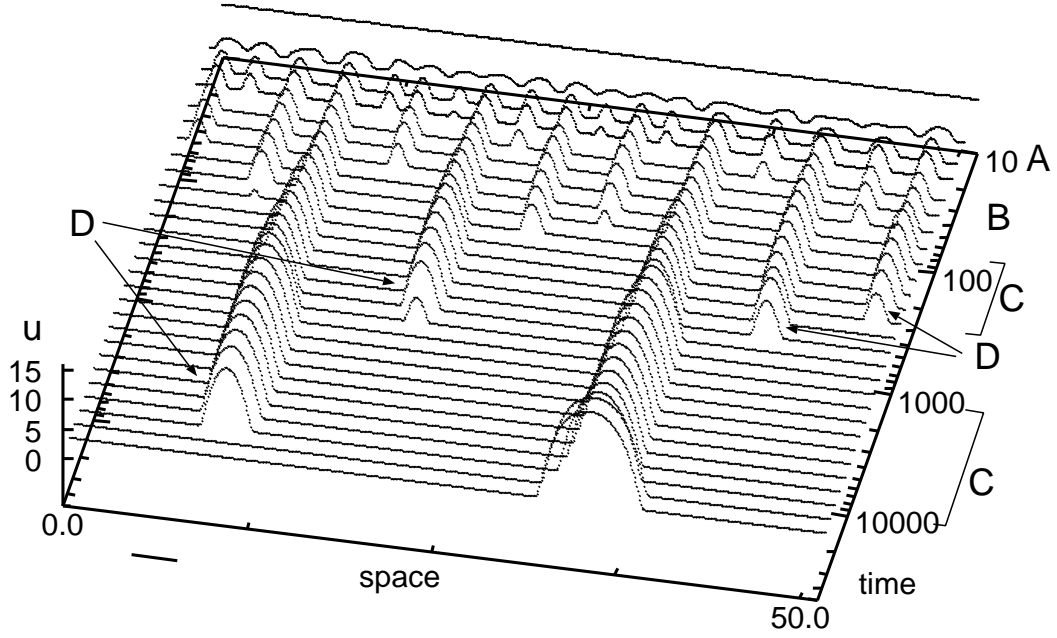


FIG. 1: Transient dynamics of a mass-conserved system. The model system and the meaning of alphabet letters are explained in the text. System size was chosen as $L = 50.0$ here. Note that time scale is represented by log scale. In the system, the most unstable wavelength at homogeneous state is $\ell_m = 3.2$, shown by the line segment in the left bottom. We checked that the system eventually falls to a one-stripe pattern for any system size between $2.0 \leq L \leq 100.0$.

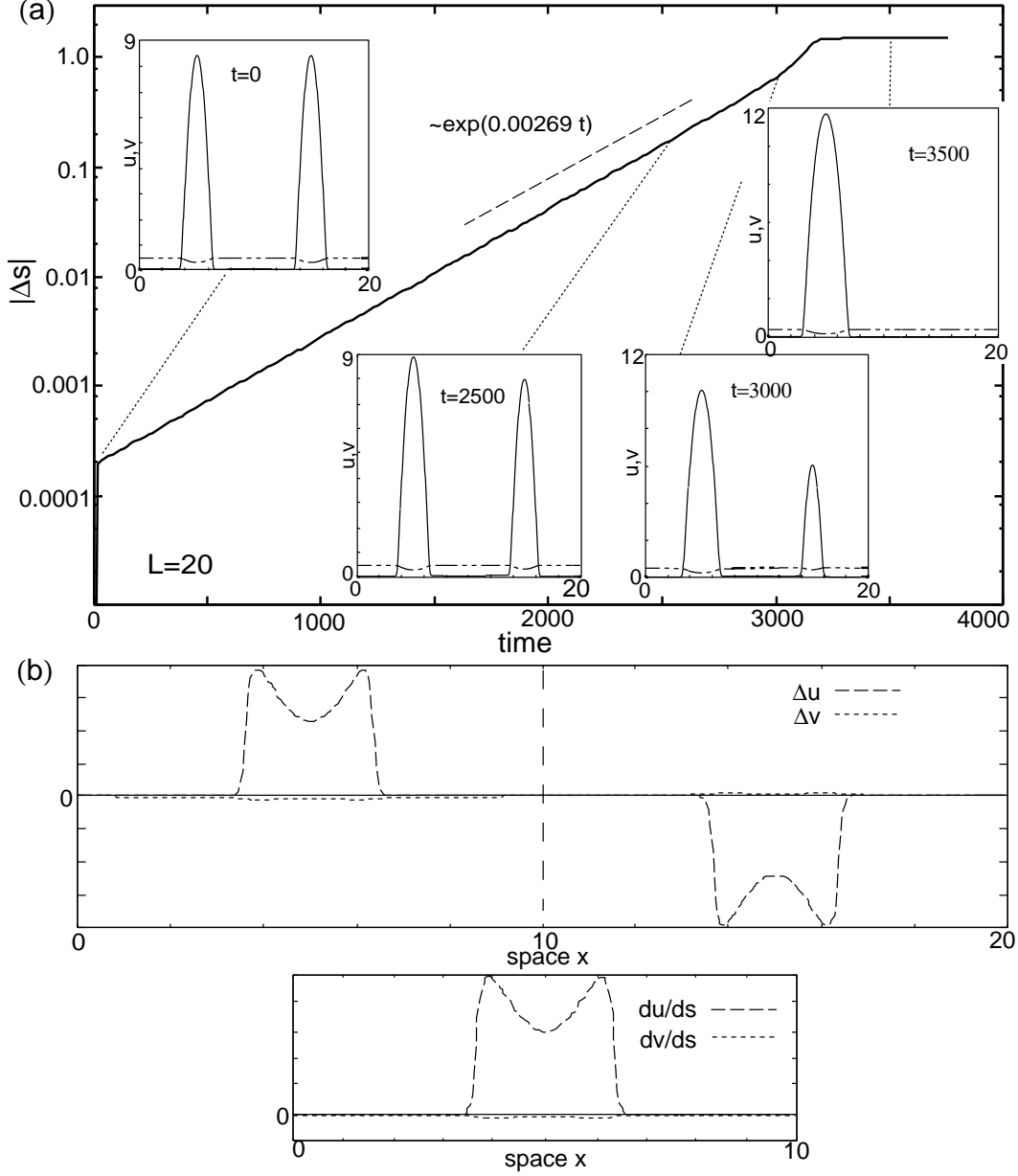


FIG. 2: Two identical steady solutions for $\frac{L}{2} = 10.0$ are connected and perturbed ($\pm 1.0\%$, keeping total mass quantity) at $t = 0$. (a) $|\Delta s|$ grows exponentially with time, indicating that one stripe decays while the other grows. $u(x, t)$ (solid) and $v(x, t)$ (broken) at $t = 0, 2500, 3000$ and 3500 are shown in insets. (b) $\Delta \vec{w}(x)$, the difference of $\vec{w}(x, t)$ between $t = 200$ and 300 is shown in the top panel, while $\partial_s \vec{w}_0$ is shown in the bottom panel (normalization is applied).

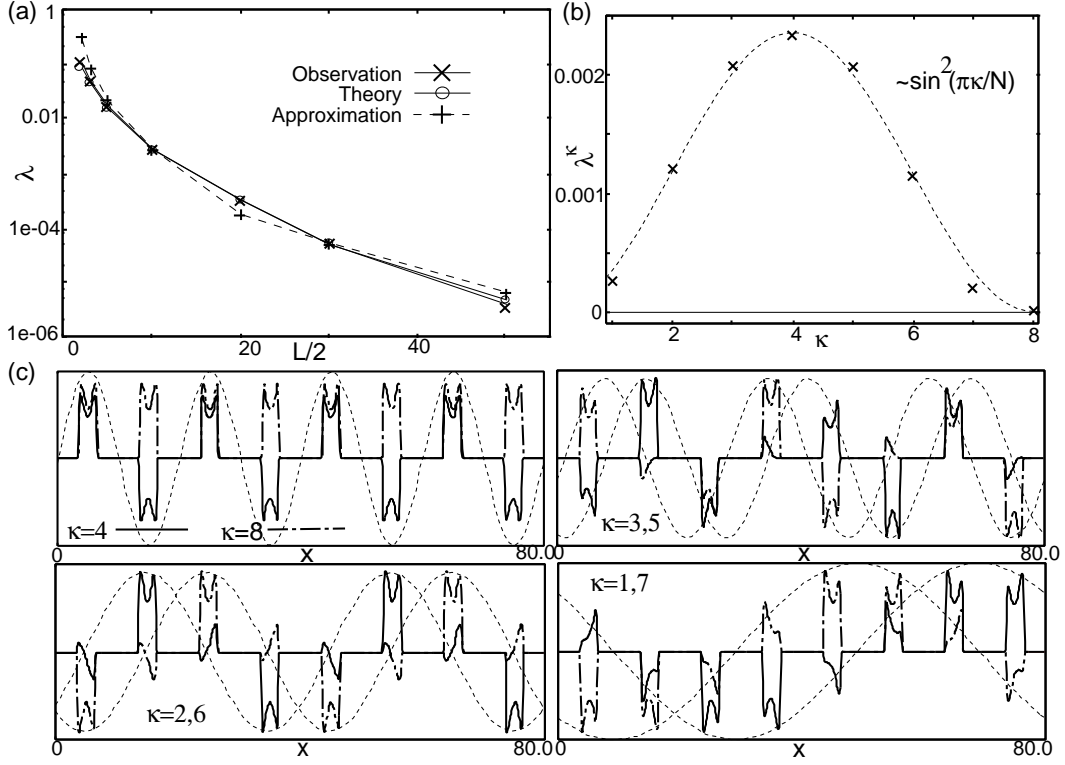


FIG. 3: (a) Growth rates λ for respective system sizes are evaluated from the observations of $|\Delta s(t)|$ (\times) and from Eq. (13) (\circ). Approximated estimation of λ , $-\frac{4}{L^2}\partial_s P$, are also plotted ($+$). (b) Eigen values of \mathcal{L} for the 8-stripe state are numerically calculated ($L = 80.0$), and (c) corresponding eigen functions. Note that eigen values except $\kappa = 4, 8$ are degenerated. Sinusoidal curves are also shown for guidance.